Experimental Demonstration of Improved Neoclassical Transport with Quasihelical Symmetry

J. M. Canik, D. T. Anderson, F. S. B. Anderson, K. M. Likin, J. N. Talmadge, and K. Zhai
Department of Electrical and Computer Engineering, University of Wisconsin—Madison, 1415 Engineering Drive, Madison, Wisconsin 53706, USA
(Received 22 November 2006; published 23 February 2007)

Differences in the electron particle and thermal transport are reported between plasmas produced in a quasihelically symmetric (QHS) magnetic field and a configuration with the symmetry broken. The thermal diffusivity is reduced in the QHS configuration, resulting in higher electron temperatures than in the nonsymmetric configuration for a fixed power input. The density profile in QHS plasmas is centrally peaked, and in the nonsymmetric configuration the core density profile is hollow. The hollow profile is due to neoclassical thermodiffusion, which is reduced in the QHS configuration.

DOI: 10.1103/PhysRevLett.98.085002 PACS numbers: 52.55.Hc, 52.25.Fi, 52.25.Xz

In a stellarator, currents flowing in external conductors produce the confining magnetic fields. This makes the stellarator an attractive candidate for a fusion reactor, as the lack of large externally driven plasma currents lends itself to steady state, disruption-free operation. However, conventional stellarators have suffered from high neoclassical transport due to asymmetry in the magnetic field ripple, caused by the combination of toroidal and helical curvature. At low collisionality, this asymmetry gives rise to a regime in which transport increases with decreasing collisionality, leading to a heat flux that scales with temperature as $T^{9/2}$. This strong, unfavorable scaling could quickly limit the achievable plasma temperature in a reactor for a fixed power input. Although experimental transport in stellarators is generally anomalously large, neoclassical transport has been shown to be important in the core of low-collisionality plasmas [1]. Reducing this transport has been a key to achieving good confinement at such parameters [2]. In addition to large thermal transport, the asymmetric ripple of conventional stellarators is responsible for a class of particle orbits that are not confined. In a reactor, alpha particles on these direct loss orbits would leave the plasma very quickly and could cause significant wall damage.

The large low-collisionality transport in a stellarator can be greatly reduced by tailoring the magnetic field to have an approximate direction of symmetry in the magnetic field strength, a concept known as quasisymmetry [3,4]. Quasisymmetric magnetic configurations are predicted to have several advantages over conventional stellarators: neoclassical transport is reduced by as much as several orders of magnitude, viscous flow damping is reduced in the direction of symmetry, and direct loss orbits are largely eliminated. The helically symmetric experiment (HSX) [5] is the first operational stellarator based on the concept of quasisymmetry and has a helical direction of symmetry. Quasisymmetry is also the basis of the National Compact Stellarator Experiment [6], under construction, and the proposed Quasi-Poloidal Stellarator experiment [7]. A major goal of the HSX program is to test the expected improvements to neoclassical transport due to quasisymmetry.

Previously, it has been demonstrated on HSX that quasihelical symmetry results in reduced parallel viscous damping of flows in the symmetry direction [8]. In this Letter, measurements are presented of electron density and temperature profiles of plasmas produced in the quasihelically symmetric magnetic field, as well as in a field with the symmetry intentionally broken. Based on differences in these profiles, along with measurements of the corresponding source rates, we show for the first time that the reduced neoclassical transport of the quasisymmetric configuration results in significantly improved electron particle and heat confinement.

The main magnetic field of HSX is generated by a set of 48 nonplanar, modular coils, arranged in four field periods. These produce a quasihelically symmetric (QHS) field with a single dominant spectral component with mode numbers $(n, m) = (4, 1)$, where n and m are the toroidal and poloidal mode numbers, respectively. A set of auxiliary coils can be used to break the symmetry, introducing spectral terms with mode numbers $(n, m) = (4, 0)$ and $(8, 0)$. This is known as the Mirror configuration and exhibits the large neoclassical transport typical of a conventional stellarator, while the plasma volume, well depth, and rotational transform change very little.

All plasma discharges presented in this Letter are produced and heated with up to 100 kW of second harmonic X-mode electron cyclotron resonance heating (ECRH) at 28 GHz, with a magnetic field of 0.5 T. This produces low-collisionality plasmas, with a maximum density of 5×10^{12} cm^{-3} due to ECRH cutoff. Electron density and temperature profiles are measured using a Thomson scattering system with 10 spatial channels [9]. The density measurement is corroborated by a 9-channel microwave interferometer [10]. Measurements using Doppler spectroscopy indicate impurity ion temperatures of 20–30 eV in both the QHS and Mirror configurations.

The neoclassical transport coefficients in the QHS and Mirror configurations are obtained using the DKES code

[11,12]. DKES calculates the monoenergetic diffusion coefficient for a given magnetic configuration as a function of collisionality and radial electric field. The neoclassical particle and heat fluxes are given by

$$\Gamma_s = -n_s\left[D_{11}^s\left(\frac{\nabla n_s}{n_s} - \frac{q_s E_r}{T_s}\right) + D_{12}^s\frac{\nabla T_s}{T_s}\right], \quad (1a)$$

$$Q_s = -n_s T_s\left[D_{21}^s\left(\frac{\nabla n_s}{n_s} - \frac{q_s E_r}{T_s}\right) + D_{22}^s\frac{\nabla T_s}{T_s}\right], \quad (1b)$$

where n is plasma density, T is the temperature, q is particle charge, E_r is the radial electric field, and the label s denotes particle species. The coefficients D_{11}, D_{12}, D_{21}, and D_{22} are obtained by integrating the energy-weighted monoenergetic diffusion coefficient over a Maxwellian distribution [11]. The electric field is calculated from the roots of the ambipolarity condition of the neoclassical particle fluxes: $\Gamma_e = \Gamma_i$.

Electron temperature and density profiles are routinely measured in HSX plasmas. For a fixed ECRH power level, two important differences in these profiles are observed between the QHS and Mirror configurations: the temperature is substantially higher in QHS, and the density profile in QHS is centrally peaked, compared to a hollow profile in the core of the Mirror configuration. The total transport is a combination of neoclassical and anomalous components. Since the level of anomalous transport may depend on the temperature, these discharges are not ideal for comparing measured transport differences to neoclassical calculations. A better comparison is made with discharges in which the temperature profiles in the two configurations are matched by changing the input power. This is achieved by heating the QHS plasma with 26 kW of injected power, and the Mirror plasma with 67 kW; these plasmas are the focus of this Letter. The density and temperature profiles for this scenario are shown in Fig. 1. The density in the two configurations cannot be matched as closely, due to the very different profile shapes.

The hollow density profile observed in the Mirror configuration is typical of stellarators heated with central ECRH deposition [13–16]. In steady state, the hollow density profile requires an outward convective particle flux to balance the inward flux due to the density gradient. To study this, the experimental particle flux has been inferred using a set of absolutely calibrated H_α detectors [17], coupled to 3D neutral gas modeling using the DEGAS code [18]. The measured flux is shown in Fig. 2(a) for the Mirror discharge. Also shown is the neoclassical particle flux, which is separated into the fluxes driven by the

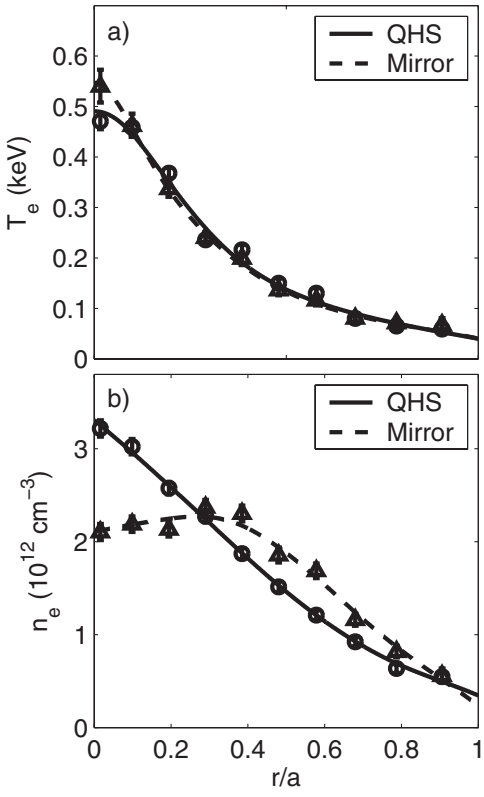

FIG. 1. Profiles of (a) electron temperature and (b) density for a QHS plasma with 26 kW of injected power and a Mirror plasma with 67 kW of power.

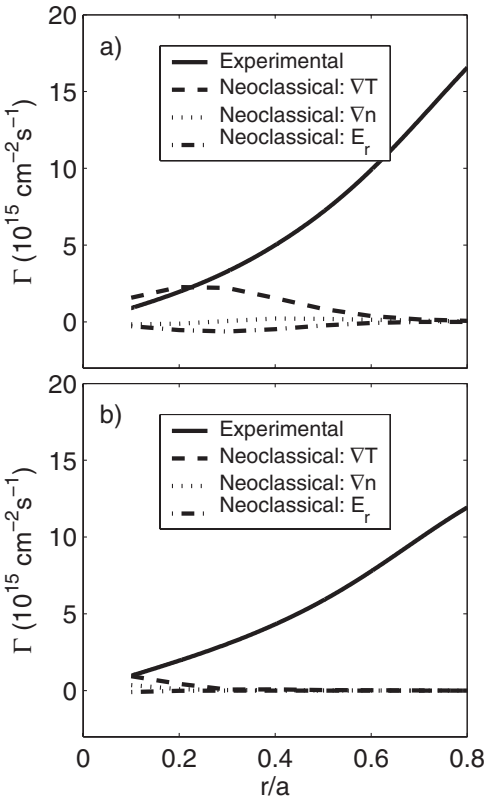

FIG. 2. Profiles of experimental and neoclassical particle fluxes for the (a) Mirror and (b) QHS discharges shown in Fig. 1. The neoclassical flux is broken into the components driven by the density and temperature gradients and the radial electric field.

density gradient, electric field, and temperature gradient [see Eq. (1a)]. From the figure it can be seen that the thermodiffusive component of the flux is dominant. Inside a normalized radius of ~0.3, the experimental particle flux in the Mirror configuration is close to the neoclassical flux driven by the temperature gradient. This corresponds to the region in which the density profile shows a clear flattening as compared to the QHS profile. Thus, the hollow density profile observed in the Mirror configuration is caused by neoclassical thermodiffusion. Off-axis heating experiments have confirmed the thermodiffusive flux in Mirror; when the ECRH resonance is moved off axis, the core temperature profile is flattened (eliminating thermodiffusion), and peaked density profiles are observed. An example of this can be seen in Fig. 3, which shows the temperature and density profiles for a Mirror plasma in which the ECRH resonance is located at a minor radius of $r/a \sim 0.3$.

In the case of the QHS plasma, however, the density profile is centrally peaked. This is due to the reduction in neoclassical transport in the quasisymmetric magnetic field; the neoclassical thermodiffusive flux is not large enough in QHS to cause the density profile to be hollow. This is illustrated in Fig. 2(b), which shows the experimental and neoclassical fluxes for the QHS case. As can be seen, the neoclassical flux is much less than the experimental value across the minor radius of the plasma. In the outer region of the plasma, where the experimental particle flux is much larger than neoclassical in both QHS and Mirror, the experimental fluxes in the two configurations are comparable in magnitude. This indicates that the anomalous component of the total particle transport is similar in the two configurations.

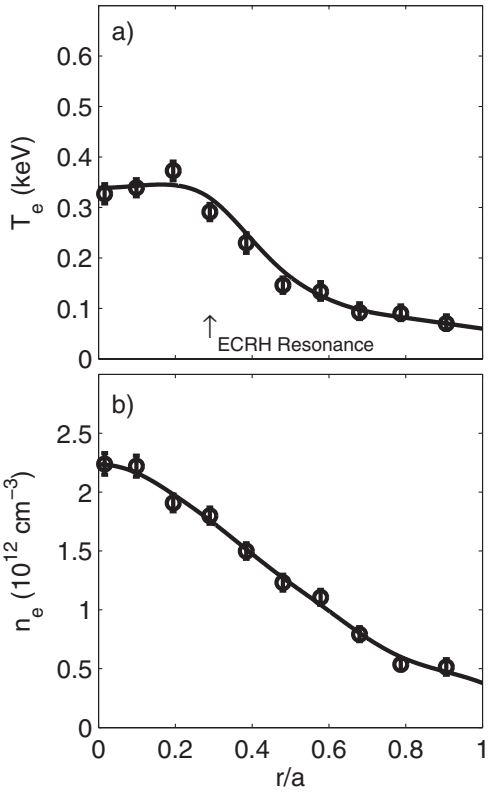

FIG. 3. Profiles of the (a) electron temperature and (b) density profile for a Mirror plasma in which the power is deposited off axis.

In all HSX discharges, atomic hydrogen penetrates throughout the plasma. This is due to the low plasma densities and small minor radius of the machine. As a result, a significant particle source exists in the core of the plasma, and the peaked density profile in QHS can be understood in terms of purely diffusive anomalous transport, without the need to invoke an inward particle pinch. In a large stellarator with higher density plasmas, the particle source will be localized to the edge. In this case, peaked density profiles will be possible only with an additional inward pinch. Without this pinch, and assuming that diffusion continues to be anomalously large, the reduced neoclassical transport in a quasisymmetric device would lead a less hollow density profile than in a conventional stellarator, but not a peaked profile such as observed in the QHS configuration.

Analysis of the electron heat transport has been performed for the discharges shown in Fig. 1. In this analysis, a model profile shape for the power absorption has been used, and the total power is taken from experimental measurements. The shape of the absorbed power profile is based on ray tracing calculations, which show very centrally peaked power deposition, with negligible difference in shape between the QHS and Mirror cases. The ray tracing calculations indicate 9 kW of absorbed power in the QHS case, and 14 kW in Mirror. Measurements of the total absorbed power have been performed by analyzing the decay of the plasma stored energy after the ECRH switch-off, as is commonly done using diamagnetic loops to measure the stored energy. However, at high power levels, HSX plasmas have a large population of suprathermal electrons, which contaminate the measurement of both the plasma energy and absorbed power using the diamagnetic loop [19]. This effect is larger in the Mirror case, due to the higher injected power. For this reason, the Thomson scattering system is used to measure the absorbed power; the kinetic stored energy from the density and temperature profiles is measured over many similar discharges, with the timing of the Thomson measurement changed from just before to just after the ECRH turn-off. Because the Thomson scattering measurement is relatively insensitive to the fast electrons, this yields the power absorbed by the bulk plasma, rather than by tail electrons. The absorbed power is measured to be 10 kW in the QHS case and 15 kW in Mirror, in good agreement with the ray tracing calculations. Because of the efforts to match the profiles in QHS and Mirror, the total stored energy in both configurations is 17 J. Thus, the QHS plasma has a sub-

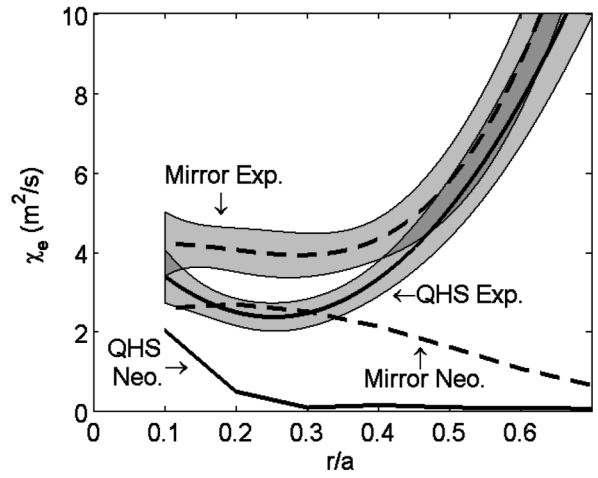

FIG. 4. Experimental and neoclassical thermal diffusivities for QHS and Mirror plasmas.

stantially longer energy confinement time of 1.7 ms, compared to 1.1 ms in Mirror.

A purely conductive ansatz is used in the analysis of electron heat transport, with $Q_e = -n_e \chi_e \nabla T_e$. This is valid inside a minor radius of $r/a \sim 0.6$, where convection, radiation, and electron-ion energy transfer are a small part of the total power balance. The results of this analysis are shown in Fig. 4, where the experimental electron thermal diffusivity χ_e is shown in the plasma core. The shaded regions in the graph indicate the error in the measurement, which comes from both the error in the measurement of the temperature profiles and the error in the kinetic measurement of the absorbed power. Also shown are the neoclassical values of the electron thermal diffusivity for the two configurations. It can be seen from this figure that transport in the outer regions of the two plasmas is much larger than neoclassical, and the error in the measurement overcomes any difference in the values of χ_e between QHS and Mirror in this region. Inside a normalized radius of $r/a \sim 0.4$, however, the experimental transport in the QHS configuration is clearly reduced compared to Mirror. At $r/a \sim 0.2$–0.3, the experimental value of χ_e is just above 2 m^2/s in QHS and $\sim$4 m^2/s in Mirror. The magnitude of the reduction in the experimental χ_e in QHS compared to Mirror is comparable to the reduction in the neoclassical value, which is $\sim$2.5 m^2/s in the same region.

In the Mirror plasma being discussed, the neoclassical ambipolarity constraint yields large, positive radial electric fields, the so-called "electron root" [20]. This strong electric field reduces the neoclassical transport by one to 2 orders of magnitude in Mirror, whereas the electric field has very little effect in QHS. Operating with the plasma in the electron root is another method of reducing low-collisionality stellarator transport other than quasisymmetry, and has proven effective in reducing core transport [21]. However, the electric field is ineffective in reducing alpha particle loss. The results discussed in this Letter demonstrate the effectiveness of quasisymmetry in reducing neoclassical transport, even when compared to an electron-root scenario in the Mirror configuration.

In summary, quasisymmetry has been observed to have a strong effect on plasma profiles in HSX. Measurements have been made of the particle source rate and absorbed power, and transport analysis shows that the profile differences are due to the improved neoclassical properties of the quasisymmetric configuration. The reduction in neoclassical thermodiffusion causes the density profile to be centrally peaked with quasisymmetry, in contrast to the hollow profiles observed when the symmetry is broken. Improved electron thermal transport is also observed; transport analysis on discharges with matched temperature profile show that the experimental reduction in transport in QHS is comparable to the neoclassical calculation. These results demonstrate for the first time reduced particle and heat transport due to low neoclassical transport with quasisymmetry.

The authors would like to thank L. Owen, D. Spong, S. P. Hirshman, and Oak Ridge National Laboratory for providing the DEGAS and DKES codes. We also gratefully acknowledge the assistance of C. Clark, C. Deng, W. Guttenfelder, M. Frankowski, E. Jolitz, A. Piccione, and P. Probert. This work was supported by the U.S. Department of Energy under Contract No. DE-FG02-93ER54222.

[1] H. Maassberg *et al.*, Phys. Fluids B **5**, 3627 (1993).
[2] O. Motojima *et al.*, Nucl. Fusion **43**, 1674 (2003).
[3] J. Nuhrenberg and R. Zille, Phys. Lett. A **129**, 113 (1988).
[4] D. A. Garren and A. H. Boozer, Phys. Fluids B **3**, 2822 (1991).
[5] F. S. B. Anderson *et al.*, Fusion Technol. **27**, 273 (1995).
[6] G. H. Neilson *et al.*, J. Plasma Fusion Res. **78**, 214 (2002).
[7] D. A. Spong *et al.*, Nucl. Fusion **41**, 711 (2001).
[8] S. P. Gerhardt, J. N. Talmadge, J. M. Canik, and D. T. Anderson, Phys. Rev. Lett. **94**, 015002 (2005).
[9] K. Zhai *et al.*, Rev. Sci. Instrum. **75**, 3900 (2004).
[10] C. Deng *et al.*, Rev. Sci. Instrum. **74**, 1625 (2003).
[11] S. P. Hirshman *et al.*, Phys. Fluids **29**, 2951 (1986).
[12] W. I. van Rij and S. P. Hirshman, Phys. Fluids B **1**, 563 (1989).
[13] J. N. Talmadge *et al.*, Nucl. Fusion **29**, 1806 (1989).
[14] S. Okamura *et al.*, Nucl. Fusion **45**, 863 (2005).
[15] R. J. Colchin *et al.*, Nucl. Fusion **33**, 323 (1993).
[16] H. Maassberg *et al.*, Plasma Phys. Controlled Fusion **35**, B319 (1993).
[17] S. P. Gerhardt *et al.*, Rev. Sci. Instrum. **75**, 2981 (2004).
[18] D. Heifetz *et al.*, J. Comput. Phys. **46**, 309 (1982).
[19] K. M. Likin *et al.*, Plasma Phys. Controlled Fusion **45**, A133 (2003).
[20] H. E. Mynick and W. N. G. Hitchon, Nucl. Fusion **23**, 1053 (1983).
[21] M. Yokoyama *et al.*, Fusion Sci. Technol. **50**, 327 (2006).